Neural sliding-mode load frequency controller design of power systems

Dianwei Qian, Dongbin Zhao, Jianqiang Yi & Xiangjie Liu

Neural Computing and Applications

ISSN 0941-0643
Volume 22
Number 2

Neural Comput & Applic (2013)
22:279-286
DOI 10.1007/s00521-011-0709-0

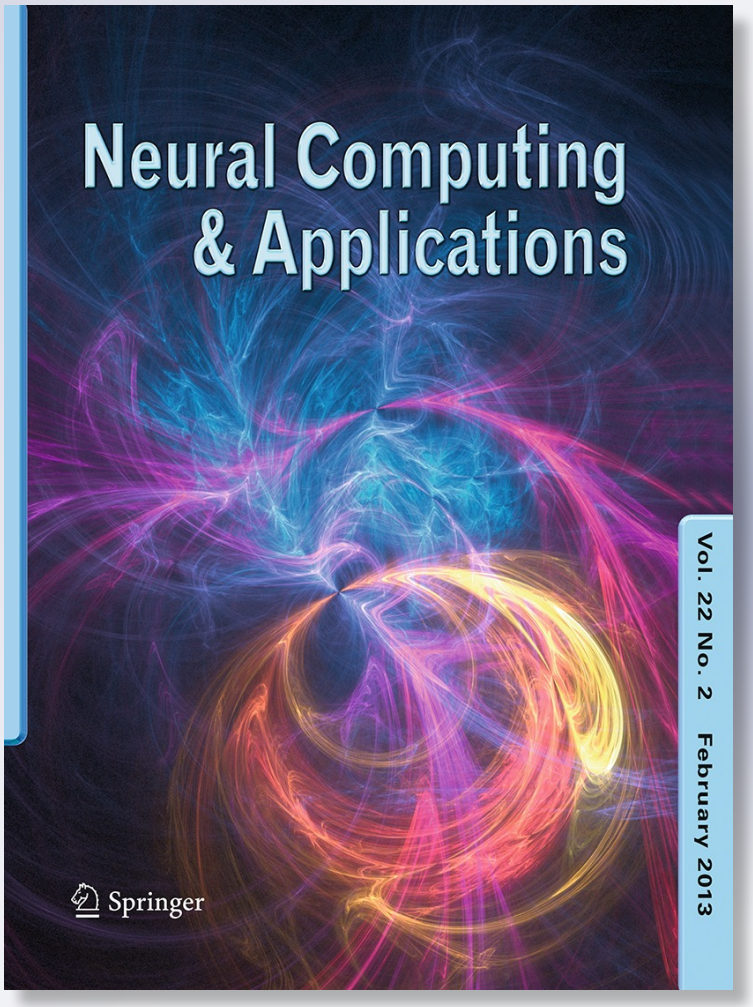

Springer

Neural Comput & Applic (2013) 22:279–286
DOI 10.1007/s00521-011-0709-0

ISNN 2011

Neural sliding-mode load frequency controller design of power systems

Dianwei Qian · Dongbin Zhao · Jianqiang Yi · Xiangjie Liu

Received: 20 February 2011 / Accepted: 5 July 2011 / Published online: 22 July 2011

Abstract Load frequency control (LFC) is one of the most profitable ancillary services of power systems. Governor dead band (GDB) nonlinearity is able to deteriorate the LFC performance. In this paper, controller design via a neural sliding-mode method is investigated for the LFC problem of power systems with GDB. Power systems are made up of areas. In each area, a sliding-mode LFC controller is designed by introducing an additional sate, and a RBF neural network is utilized to compensate the GDB nonlinearity of the area. Weight update formula of the RBF network is derived from Lyapunov direct method. By this scheme, not only the update formula is obtained, but also the control system possesses the asymptotic stability. Simulation results illustrate the feasibility and robustness of the presented approach for the LFC problems of single-area and multi-area power systems.

D. Qian (✉) · X. Liu
School of Control and Computer Engineering,
North China Electric Power University,
Beijing 102206, People's Republic of China
e-mail: dianwei.qian@ncepu.edu.cn

X. Liu
e-mail: liuxj@ncepu.edu.cn

D. Zhao
State Key Laboratory for Intelligent Control and Management of Complex Systems, Institute of Automation,
Chinese Academy of Sciences, Beijing 100190,
People's Republic of China
e-mail: dongbin.zhao@ia.ac.cn

J. Yi
Institute of Automation, Chinese Academy of Sciences,
Beijing 100190, People's Republic of China
e-mail: Jianqiang.yi@ia.ac.cn

Keywords Load frequency control · Sliding-mode control · Governor dead band (GDB) · Compensator design · Neural networks

1 Introduction

Operation of power systems requires matching the total generation with the total load demand and with the associated system losses [1]. To achieve this goal, load frequency control (LFC) is introduced. In practice, LFC is one of the most important issues in power system design and operation for supplying sufficient and reliable electric power with good quality. The main objective of LFC is to control the real power output of generating units in response to changes in system frequency and tie-line power interchange within specified limits [2].

With the increasing of complexity of modern power systems, applications of advanced control methods on the LFC problem have been reported in the last decade, e.g., optimal control [3], adaptive control [4], robust control [5, 6], intelligent control [7], internal model control [8, 9], predictive control [10], etc. See [11] for a complete review of recent philosophies in LFC control strategies. Sliding-mode control (SMC) is a form of variable structure control [12]. Due to its robust behavior in controlling systems with external disturbances and parameter variations, SMC imposes as a possible choice to solve the LFC problem. In [13, 14], two variable structure control methods are investigated for the LFC problems of multi-area and single-area power systems, respectively. Recently, SMC has been paid more and more attentions to deal with the LFC problem of power systems [15, 16].

As far as power system models are concerned, a linear model around a nominal operating point is usually used in

the LFC controller design. However, power system components are inherently nonlinear, so the implementation of LFC strategies based on a linearized model on an essentially nonlinear system does not necessarily ensure the stability of the system [11]. As Tripathy [17] pointed out, the effects of these nonlinearities tend to produce continuous oscillations in the area frequency and tie-line power transient response. For the LFC problem, the nonlinearities of governor dead band (GDB) and generation rate constraint (GRC) are usually involved. A common technology to handle the nonlinearities is to design a controller for the linear nominal system; then, the linear model-based controller is directly imposed on the nonlinear system [16–20]. Although this methodology may work, the system stability cannot be theoretically ensured, the system robustness will be definitely decreased, and the system performance may be badly deteriorated. To overcome GRC, Tan in [6] presented a kind of anti-GRC structure. But so far, there has been no literature about how to overcome the GDB problem. Especially, concerning the applications of SMC on LFC [13–16], only Vrdoljak et al. [16] considered the effect of the GDB nonlinearity, where their linear model-based controller was directly applied to the nonlinear system. Although their simulation results displayed the controller's feasibility, a series of drawbacks may be induced because the linear model-based controller has no ability to deal with GDB in reality. To turn SMC into practical accounts on LFC, it is necessary to approximate and compensate the GDB nonlinearity of LFC.

It is proven that the methodology of radial basis function (RBF) neural networks (NNs) is a universal approximator [21]. In [22], a gradient-type method on basis of RBF NNs is proposed to deal with the dead band nonlinearity. So far, there has been rare literature about employing sliding-mode-based RBF NNs to compensate the GDB problem of LFC. In this paper, a sliding-mode controller is developed for the LFC problem of a linear power system at first. Then, a sliding-mode-based RBF NN compensator is designed to compensate the nonlinearity of GDB. Weight update formula of the network is deduced from Lyapunov direct method, so the weight convergence and system stability are simultaneously guaranteed in the sense of Lyapunov scheme. Finally, simulation results show the feasibility and robustness of the presented method for the LFC problems of nonlinear single-area and multi-area power systems.

2 System model

The power system for the LFC problem under consideration is expressed only to relatively small changes, so it can be adequately represented by the linear models of governor, turbine, and power system in Fig. 1. Figure 1 represents the block diagram of a single-area power system with the GDB nonlinearity. Note that the generating unit in Fig. 1 means all units in the prescribed area are lumped together. The symbols in Fig. 1 are explained as Laplace operator s, speed regulation due to governor action R (Hz/p.u.MW), governor time constant T_g (s), turbine time constant T_t (s), electric system time constant T_p (s), electric system gain K_p, incremental frequency deviation $\Delta f(t)$ (Hz), incremental change in generator output $\Delta P_g((t)$ (p.u.MW), load disturbance $\Delta P_d(t)$ (p.u.MW), incremental change in governor valve position $\Delta X_g(t)$, control input produced by the designed LFC controller $u(t)$. In state space, to force the steady state of $\Delta f(t)$ to tend to zero, the integral of $\Delta f(t)$ is introduced as an additional state [5], defined as

$$\mathscr{L}[\Delta E(t)] = \frac{K_e}{s}\mathscr{L}[\Delta f(t)] \tag{1}$$

where K_e is gain of the additional state, $\mathscr{L}[\cdot]$ means Laplace transform. It is obvious that the system consists of three parts:

- Turbine with dynamics $G_t(s) = \frac{1}{T_t s+1}$
- Generator with dynamics $G_g(s) = \frac{1}{T_g s+1}$
- Electric power system with dynamics $G_p(s) = \frac{K_p}{T_p s+1}$

3 Control design

Due to the difficulties of designing a controller for the theoretically stable system with GDB in Fig. 1, the following technical route is going to be adopted. We will

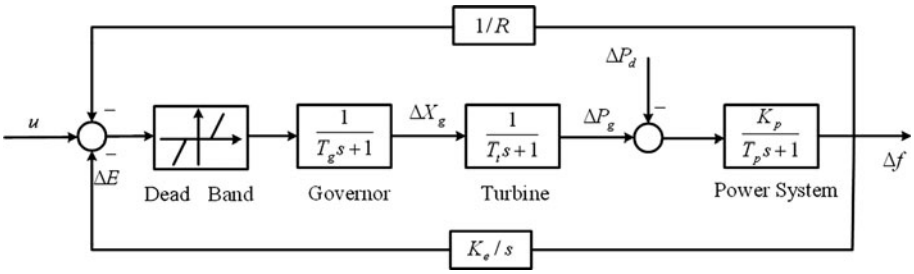

Fig. 1 Diagram of a single-area power system with the GDB nonlinearity

develop a SMC controller for the linear system with no GDB at first. But the linear model-based controller may deteriorate the performance of the real nonlinear system shown in Fig. 1. To achieve the LFC objective, it is desired to solve the issue. Then, a sliding-mode-based neural compensator is proposed to compensate the GDB nonlinearity of the real nonlinear system. At last, the controller designed for the linear power system and the compensator for GDB will work together to realize the LFC objective of the nonlinear power system.

3.1 Design of sliding-mode controller

The linear system with no GDB shown in Fig. 1 involves four state variables, i.e., $\Delta P_g, \Delta X_g, \Delta f$ and ΔE. The state equation of the linear system is depicted as

$$\dot{\mathbf{x}}(t) = A\mathbf{x}(t) + Bu(t) + Fd(t) \tag{2}$$

where $\mathbf{x} = [\Delta f\ \Delta P_g\ \Delta X_g\ \Delta E]^T$ is state vector, u is LFC control input, d is load disturbance, A is a 4×4 system matrix, B is a 4×1 input matrix, and F is a 4×1 disturbance matrix.

$$A = \begin{bmatrix} -\frac{1}{T_p} & \frac{K_p}{T_p} & 0 & 0 \\ 0 & -\frac{1}{T_t} & \frac{1}{T_t} & 0 \\ -\frac{1}{RT_g} & 0 & -\frac{1}{T_g} & -\frac{1}{T_g} \\ K_e & 0 & 0 & 0 \end{bmatrix} \quad B = \begin{bmatrix} 0 \\ 0 \\ \frac{1}{T_g} \\ 0 \end{bmatrix}$$

$$F = \begin{bmatrix} \frac{K_p}{T_p} \\ 0 \\ 0 \\ 0 \end{bmatrix}$$

The control objective of LFC is to keep the change in frequency Δf as close to 0 as possible when the system is subjected to a load disturbance d by manipulating the input u. Here, we employ the SMC technology to achieve this goal. At first, a sliding surface is defined as

$$S = c^T\mathbf{x} \tag{3}$$

here c is a 4×1 constant matrix. Usually, the SMC law is made up of two parts, equivalent control and switching control [12]. We differentiate S with respect to time t and let $\dot{S} = 0$. The equivalent control law u_{eq} can be gotten as

$$u_{eq} = -(c^TB)^{-1}c^TA\mathbf{x} \tag{4}$$

Then, substituting (4) into (2), we can have c by Ackermann's formula [12]. Define a Lyapunov function $V = \frac{S^2}{2}$, define the total SMC law u as $u_{eq} + u_{sw}$ (here u_{sw} is the switching control law), differentiate V with respect to time t, substitute (2), (3), (4) into $\dot{V}$, then, we are able to obtain u_{sw} from $\dot{V} < 0$ as

$$u_{sw} = -(c^TB)^{-1}[KS + \eta\mathrm{sgn}(S)] \tag{5}$$

where K and η are positive constants, $\mathrm{sgn}(\cdot)$ means sign function. On the aspect of system stability, we choose $\eta > c^TF\bar{d}$, here $\bar{d} = \sup d(t)$. Finally, the total SMC law u for the linear model can be obtained by u_{eq} plus u_{sw}.

3.2 Design of neural compensator

Due to RBF NNs owning the ability to approximate complex nonlinear mapping directly from input–output data with a simple topological structure [21], we will adopt such the kind of NNs to realize the compensator design. In Fig. 2, a RBF NN with the input u^* and the output Δu^* is utilized to compensate the dead band of the system, where u^* and $\Delta\tau^*$ are defined as $u - \Delta E - \frac{\Delta f}{R}$ and $u^* + \Delta\hat{u}^*$, respectively.

Define a nonlinear function $D(\cdot)$ as $\Delta\tau = D(\Delta\tau^*)$ to depict the dead band nonlinearity in Fig. 2; then, the inverse of the dead band nonlinearity D^{-1} is able to be obtained as

$$D^{-1}(u^*) = u^* + \Delta u^* \tag{6}$$

here Δu^* is the desired output of the neural network. From (6), Δu^* can be obtained as $\Delta u^* = D^{-1}(u^*) - u^*$. This case inspires us to approximate D by utilizing the properties of NNs. In Fig. 2, it is obvious that $\Delta\hat{u}^*$ is the estimated value of D. Thus, the network output is determined as

$$\Delta\hat{u}^* = \mathbf{w}_c{}^T\Phi_c(u^*) \tag{7}$$

here $\mathbf{w}_c \subseteq R^{n_c \times 1}$ is the weight vector of the RBF network, where n_c is the number of the hidden neurons, $\Phi_c(u^*) = [\phi_{c1}(u^*), \phi_{c2}(u^*), \ldots, \phi_{cn_c}(u^*)]^T$ is a radial basis function vector where the kth RBF function of the network is determined as

$$\phi_{ck}(u^*) = \exp\left(-\frac{||u^* - \gamma_{ck}||^2}{\delta_{ck}^2}\right) \tag{8}$$

here γ_{ck} and δ_{ck} depict the center and width of the kth hidden neuron of the network, respectively. For the further analysis, we have the following assumption.

Assumption 1 There exists an optimal weight vector $\mathbf{w}_{co}$, so the network output satisfies $|\mathbf{w}_{co}{}^T\Phi(u^*) - \mathbf{w}_c{}^T\Phi(u^*)| < \epsilon_c$, where ϵ_c is a positive constant.

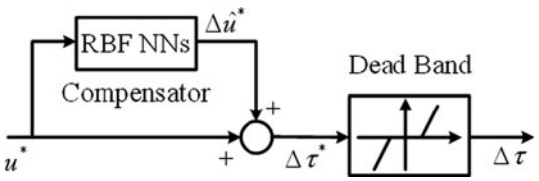

Fig. 2 Diagram of RBF NNs to compensate the GDB nonlinearity

Theorem 1 *Consider the nonlinear system as Fig. 1, design the SMC controller as (4) and (5), compensate the GDB as Fig. 2. If the update formula of the network weight* $\mathbf{w}_c$ *in Fig. 2 is adopted as*

$$\dot{\mathbf{w}}_c = \alpha \cdot S^2 \cdot \Phi_c(u^*) \tag{9}$$

here α is a positive constant, then, the control system is of asymptotic stability.

Proof Define $\tilde{\mathbf{w}}_c = \mathbf{w}_{\mathrm{co}} - \mathbf{w}_c$ as the weight error of the network, so we have $\dot{\tilde{\mathbf{w}}}_c = -\dot{\mathbf{w}}_c$. Then, we define another Lyapunov function (10) to deduce the update formula of the network.

$$V_n = \frac{S^2}{2} + \frac{\alpha^{-1}\tilde{\mathbf{w}}_c^{\mathrm{T}}\tilde{\mathbf{w}}_c}{2} \tag{10}$$

Differentiating V_n with respect to time t yields

$$\dot{V}_n = S\dot{S} + \alpha^{-1}\dot{\tilde{\mathbf{w}}}_c^{\mathrm{T}}\tilde{\mathbf{w}}_c = S\dot{S} - \alpha^{-1}\tilde{\mathbf{w}}_c^{\mathrm{T}}\dot{\mathbf{w}}_c \tag{11}$$

Substituting (2), (3), (4) and (5) into (11), we have

$$\begin{aligned}\dot{V}_n &= S\left[-KS - \eta\mathrm{sgn}(S) + c^T F d(t)\right] - \alpha^{-1}\left(\mathbf{w}_{\mathrm{co}}^T - \mathbf{w}_c^{\mathrm{T}}\right)\dot{\mathbf{w}}_c \\ &= -KS^2 - \eta|S| + c^T F d(t) S - \alpha^{-1}\left(\mathbf{w}_{\mathrm{co}}^T - \mathbf{w}_c^{\mathrm{T}}\right)\dot{\mathbf{w}}_c\end{aligned} \tag{12}$$

Substituting (9) into (12), we can obtain

$$\dot{V}_n = -KS^2 - \eta|S| + c^T F d(t) S - S^2\left(\mathbf{w}_{\mathrm{co}}^T - \mathbf{w}_c^{\mathrm{T}}\right)\Phi_c(u^*) \tag{13}$$

Further, there exists the following inequation in light of Assumption 1.

$$\begin{aligned}\dot{V}_n &< -KS^2 - \eta|S| - \epsilon_c S^2 + c^T F d(t)|S| \\ &< -KS^2 - \epsilon_c S^2 - (\eta - c^T F\bar{d})|S|\end{aligned} \tag{14}$$

In the sense of Lyapunov stability scheme, (14) indicates $\dot{V}_n < 0$, so the update formula in (9) is able to ensure the asymptotic stability of the control system with the GDB nonlinearity by employing the SMC law (4) and (5) and the sliding-mode-based neural compensation law (7). □

4 Simulation results

In this section, the presented method will be applied to LFC of a single-area power system with GDB. Typical values of the system parameters of the single-area power system [8] are determined as $K_{\mathrm{p}} = 120$, $T_{\mathrm{p}} = 20$, $T_t = 0.3$, $T_{\mathrm{g}} = 0.08$, $R = 2.4$ and $K_{\mathrm{e}} = 0.1$. Typical dead band constraint [17] is 0.06%. The parameters of the sliding surface S are gotten as $c = [0.16 \quad 0.30 \quad 0.08 \quad 3.22]^{\mathrm{T}}$ from Acker command of MATLAB by placing the pole of Ackermann's formula in the specified vector $[-1 \quad -1.3 + 2.5i \quad -1.3 - 2.5i \quad -13.3]^{\mathrm{T}}$. The switching control parameters are picked up as $K = 6$ and $\eta = 0.01$ after trial and error. γ_{ck}, the center of the k-th hidden neuron of the RBF network, is set as random number in the interval [0, 1]. The center γ_{ck} is able to be gotten by the orthogonal least square algorithm [23] as well. δ_{ck}, the width of the k-th hidden neuron of the RBF network, is set as 0.2. Other parameters α and n_c are set as 10^{-10} and 12, respectively. The initial weights of the network are set as random number in the interval $[0 \quad 10^{-4}]$. Load disturbance $d(t) = 1\%$ is applied to the system at $t = 0$.

Simulation results in Fig. 3 illustrate the feasibility of the presented control method, where the blue solid depicts the results with RBF NN compensating the dead band constraint and the black dash plots the results with no RBF NN compensator. Both the simulation results are executed by the same SMCler and load disturbance. The solitary difference between the two simulations is that one is conducted with both the compensator and the controller, and that the other is conducted by the sole controller without any compensator.

As displayed in Fig. 3, the presented approach, with the RBF NN compensator updating the network weights as (9), is able to ensure the asymptotic stability of the control system in the sense of Lyapunov. Although the curves of change of governor output ΔP and change of governor valve position ΔX almost make no difference in Fig. 3b, c, the curve of frequency deviation Δf in Fig. 3a demonstrates the superiority of the presented method on the aspect of decreasing overshoot. In Fig. 3e, the blue solid indicates the network output and the black dash means the actual value of GDB during the simulations. From Fig. 3, the designed compensator is able to partly compensate and approximate the dead band nonlinearity of power systems. In this sense, it is a sub-optimized method. But such intelligent method is able to realize robust control of this nonlinear system, and it is feasible to deal with the GDB constraint of LFC of power systems.

The simulation results in Fig. 3 are conducted for the nominal system via the SMC controller and compensator designed for the nominal system. In practice, the exact values of the system parameters are known to belong to a certain interval. To test the robustness of the presented method, the following parameter variation is taken into accounts, $\frac{1}{T_t} \in [2.564, 4.762], \frac{1}{T_{\mathrm{g}}} \in [9.615, 17.857], \frac{1}{T_{\mathrm{p}}} \in [0.033, 0.1], \frac{K_{\mathrm{p}}}{T_{\mathrm{p}}} \in [4, 12], \frac{1}{RT_{\mathrm{g}}} \in [3.081, 10.639]$. Under the robustness test, the controller and compensator parameters remain the same as the ones tuned for the nominal power system. A step load of magnitude 1% is applied at $t = 0$ for the two extreme cases. The responses are shown in Fig. 4. From Fig. 4, it is clear that the proposed method possesses good disturbance rejection performance and good robust stability against parameter variation.

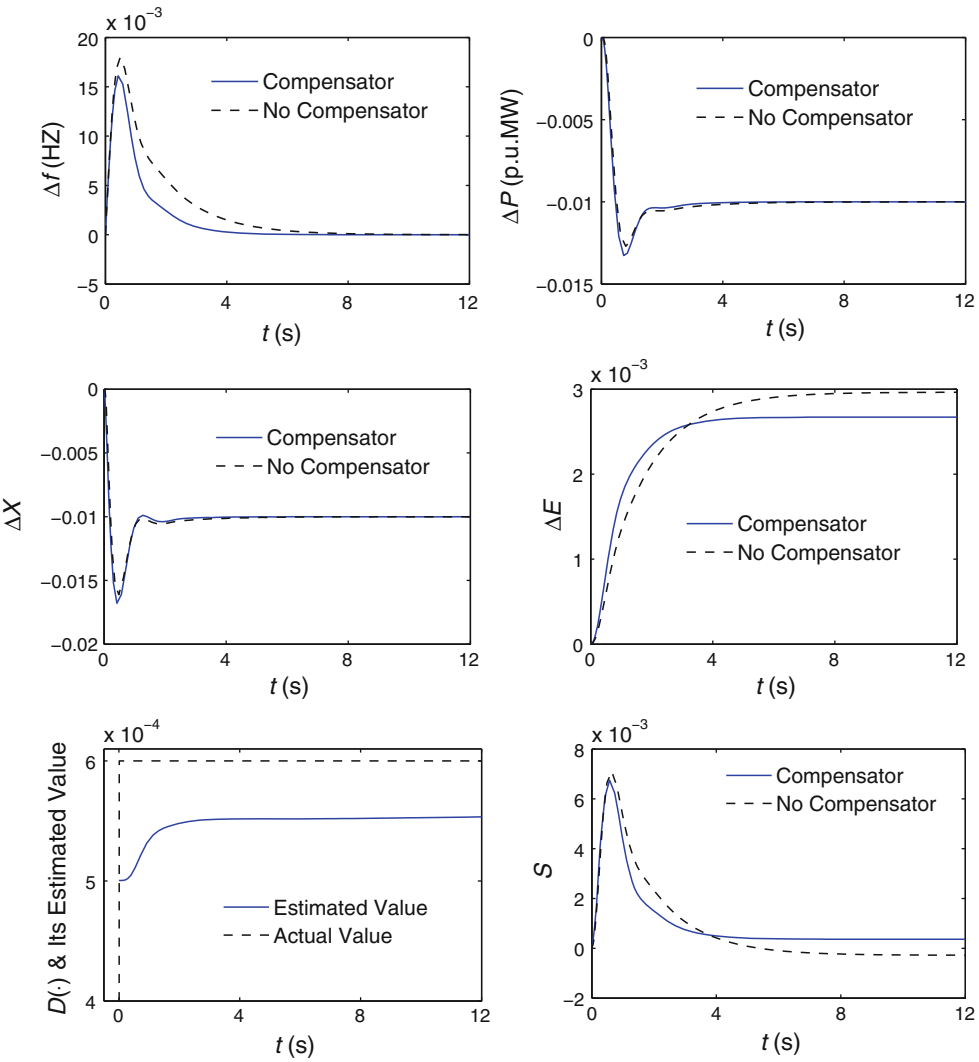

Fig. 3 Simulation results of single-area power systems. **a** Frequency deviation Δf, **b** Change of generator output ΔP, **c** change of governor valve position ΔX, **d** extra state, **e** GDB nonlinearity and its estimated value, **f** sliding surface S

5 Extensions of two-area interconnected power systems

The presented method can be extended to multi-area power systems with the GDB problem as well. Control areas interconnected each other by tie-lines consist of multi-area power systems. For the multi-area case, not only should the frequency of each control area return to its nominal value, but also the net interchange through the tie-line should return to the scheduled values. To achieve the composite goal, a new measure, named area control error (ACE), is introduced. For simplicity, a two-area interconnected power system is taken into practical accounts for the LFC problem with GDB. The model of the first control area is shown in Fig. 5.

All symbols are similar with Fig. 1, except that ΔP_{tie} is the tie-line active power deviation, T_{12} (p.u.MW) is the interconnection gain or synchronizing power coefficient between the two areas, B_1 (p.u.MW/Hz) is the frequency bias factors of the two areas, $\Delta\delta_1$ and $\Delta\delta_2$ (rad) are the rotor angle deviation of the two control areas. The ACE of the first control area, ACE_1, is defined as

$$\text{ACE}_1 = \Delta P_{\text{tie}} + B_1 \Delta f_1 \tag{15}$$

Just as the method adopted for the single-area power system model, we also introduce an additional state (16) to force the composite measure to zero.

$$\Delta \text{AS}_1 = \int K_{\text{ACE1}} \cdot \text{ACE}_1 \mathbf{d}t \tag{16}$$

here K_{ACE1} is gain of this additional state. As proven in [15, 16], the state equation of the nominal first control area with no GDB is able to be depicted as

$$\dot{\mathbf{x}}_1(t) = A_{m1}\mathbf{x}_1(t) + B_{m1}u_1(t) + F_{m1}d_1(t) \tag{17}$$

where $\mathbf{x}_1 = [\Delta f_1\ \Delta P_{g1}\ \Delta X_{g1}\ \Delta P_{\text{tie}}\ \Delta \text{AS}_1]^T$ is state vector, u_1 is LFC control input of the first control area, A_{m1} is a 5×5 system matrix, B_{m1} is a 5×1 input matrix, F_{m1} is a 5×1

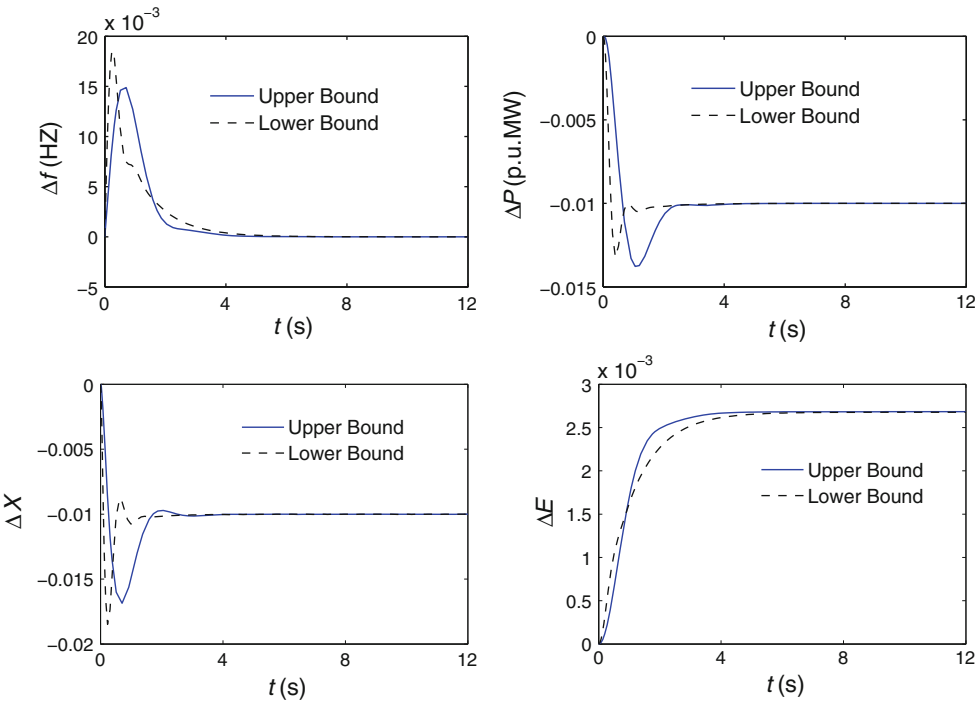

Fig. 4 Simulation results of robustness test. **a** Frequency deviation Δf, **b** change of generator output ΔP, **c** Change of governor valve position ΔX, **d** extra state

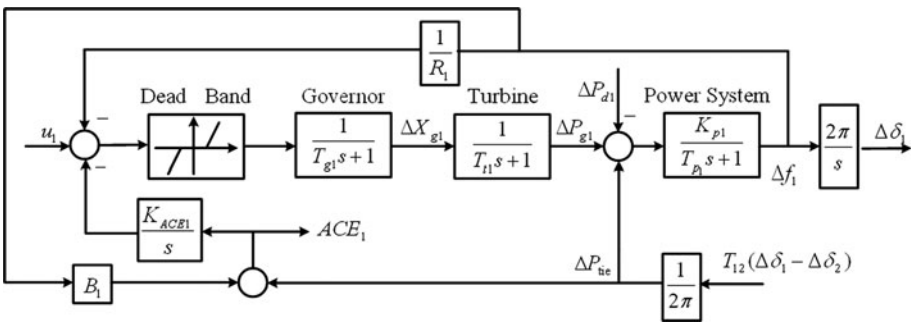

Fig. 5 Diagram of the first control area with GDB

disturbance matrix, $d_1(t)$ is load disturbance of the first control area.

$$A_{m1} = \begin{bmatrix} -\frac{1}{T_{p1}} & \frac{K_{p1}}{T_{p1}} & 0 & \frac{K_{p1}}{T_{p1}} & 0 \\ 0 & -\frac{1}{T_{t1}} & \frac{1}{T_{t1}} & 0 & 0 \\ -\frac{1}{R_1 T_{g1}} & 0 & -\frac{1}{T_{g1}} & 0 & -\frac{1}{T_g} \\ T_{12} & 0 & 0 & 0 & 0 \\ K_{ACE1} B_1 & 0 & 0 & K_{ACE1} & 0 \end{bmatrix}$$

$$B = \begin{bmatrix} 0 \\ 0 \\ \frac{1}{T_g} \\ 0 \\ 0 \end{bmatrix} \quad F = \begin{bmatrix} \frac{K_p}{T_p} \\ 0 \\ 0 \\ 0 \\ 0 \end{bmatrix}$$

Along the technical route designed in Sect. 3, the controller and compensator of the first control area are able to be obtained. For this case, the parameters of the sliding surface are obtained as $[117.7 \quad 53.0 \quad 5.6 \quad -400.3 \quad 1983.6]^{\mathrm{T}}$ from Acker command of MATLAB software by placing the pole of Ackermann's formula in the specified vector $[-26 \quad -10 \quad -5+i \quad -5-i \quad -40]^{\mathrm{T}}$. Here, the switching control parameters are picked up as $K_1 = 6$ and $\eta_1 = 0.01$. Other structure parameters in the example are determined as $K_{ACE1} = 1.00$, $T_{12} = 0.545$ and $B_1 = 0.425$. For the compensator's part, the related parameters are the same as the ones in Sect. 3. The second control area in this example is with the same structure and parameters shown in Fig. 5. It is interconnected with the first control area via the tie-line.

To show the performance of the presented method, a step load $\Delta P_{d1} = 1\%$ is applied to the system at $t = 0$ and the response curves are shown in Fig. 6. Also illustrated are the responses of the decentralized robust PID controller designed by Tan [6], where the PID controller is with the form $1.57 + \frac{2.40}{s} + 0.53s$. It is observed that the proposed approach achieves the better performance on the aspects of three key indexes, i.e., frequency deviation, tie-line scheduled power, area control error of the two control areas. The reason is due to the fact that the designed SMC

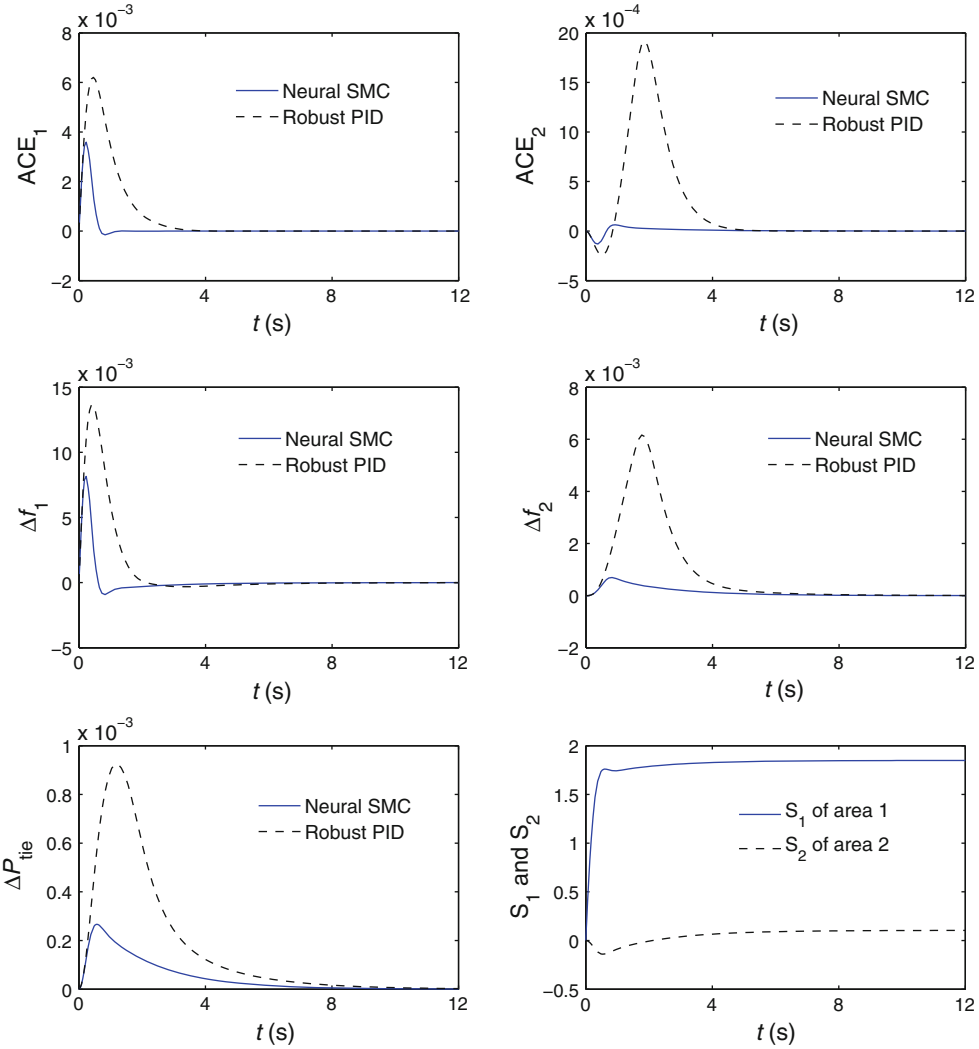

Fig. 6 Simulation results of multi-area power systems. **a** Frequency deviation Δf, **b** change of generator output ΔP, **c** change of governor valve position ΔX, **d** extra state, **e** deviation of tie-line active power ΔP_{tie}, **f** sliding surface S

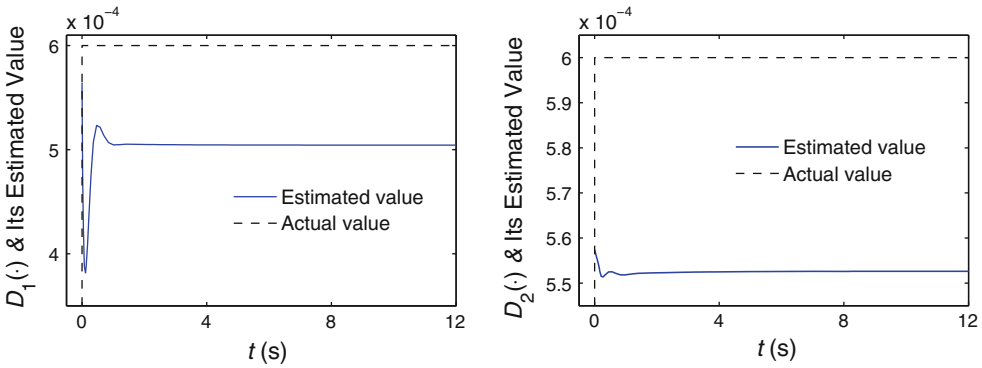

Fig. 7 Simulation results of compensator outputs. **a** Output of the first control area, **b** output of the second control area

controller is a state-based method. All the system information can be employed to improve the system performance. Further, the neural compensator is utilized to compensate the GDB nonlinearity. Both of the effects make the presented method possess a better performance. On the other hand, the robust PID controller [5] only uses the information of the frequency deviation or area control error, which makes the system performance inferior. Figure 7 displays the outputs of the neural compensators of the two control areas. It is obvious that the compensators of the two areas are able to partly compensate the system nonlinearity, just as the similar results shown in Fig. 3.

6 Conclusions

A neural SMC method for LFC of power systems with the GDB nonlinearity has been proposed. In this scheme, an additional state is introduced to the control system. Then, a sliding-mode controller is designed for the linear nominal system with no GDB, and a neural compensator is proposed to compensate GDB. The controller and compensator work together to realize robust control of the nonlinear system. The weight update formula of the network is deduced from Lyapunov direct method. It is proven that the controller and compensator are able to ensure that the control system is of asymptotic stability. Simulation results illustrate the validity and robustness of the proposed method via a single-area power system with GDB. Moreover, this method is extended to a two-area case, which demonstrates the feasibility of the presented method for LFC of multi-area interconnected nonlinear power systems.

Acknowledgments This work was supported by the NSFC Projects under grants No. 60904008, 60874043, 60921061, 61034002, 60975060, the Fundamental Research Funds for the Central Universities under grant No. 09MG19.

References

1. Kundur P (1994) Power system stability and control. McGraw-Hill, New York
2. Kothari DP, Nagrath IJ (2003) Modern power system analysis, 3rd edn. McGraw-Hill, Singapore
3. Ibraheem, Kumar P (2004) A novel approach to the matrix Riccati equation solution: an application to optimal control of interconnected power systems. Electr Power Compon Syst 32(1):33–52
4. Zribi M, Al-Rashed M, Alrifai M (2005) Adaptive decentralized load frequency control of multi-area power systems. Int J Electr Power Energy Syst 27(8):575–583
5. Tan W, Xu Z (2009) Robust analysis and design of load frequency controller for power systems. Electr Power Syst Res 79(5):846–853
6. Tan W (2009) Tuning of PID load frequency controller for power systems. Energy Convers Manage 50(4):1465–1472
7. Çam E (2007) Application of fuzzy logic for load frequency control of hydroelectrical power plants. Energy Convers Manage 48(4):1281–1288
8. Tan W (2010) Unified tuning of PID load frequency controller for power systems via IMC. IEEE Trans Power Syst 25(1):341–350
9. Tan W (2011) Decentralized load frequency controller analysis and tuning for multi-area power systems. Energy Convers Manage 52(5):2015–2023
10. Liu XJ, Zhan X, Qian DW (2010) Load frequency control considering generation rate constraints. In: Proceedings of 8th world congress on intelligent control and automation, pp 1398–1401
11. Shayeghi H, Shayanfar HA, Jalili A (2009) Load frequency control strategies: a state-of-the-art survey for the researcher. Energy Convers Manag 50(2):344–353
12. Utkin VI (1992) Sliding modes in control and optimization. Springer, New York
13. Hsu YY, Chan WC (1984) Optimal variable structure controller for the load-frequency control of interconnected hydrothermal power systems. Electr Power Energy Syst 6:221–229
14. Al-Hamouz ZM, Al-Duwaish HN (2000) A new load frequency variable structure controller using genetic algorithms. Electr Power Syst Res 55(1):1–6
15. Vrdoljak K, Peric N, Mehmedovic M (2008) Optimal parameters for sliding mode based load-frequency control in power systems. In: Proceedings of international workshop on variable structure systems, pp 331–336
16. Vrdoljak K, Peric N, Petrovic I (2010) Sliding mode based load-frequency control in power systems. Electr Power Syst Res 80(5):514–527
17. Tripathy SC, Bhatti TS, Jha CS, Malik OP, Hope GS (1984) Sampled data automatic generation control analysis with reheat steam turbines and governor dead band effects. IEEE Trans Power Apply Syst 103(5):1045–1051
18. Lu CF, Liu CC (1995) Effect of battery energy storage system on load frequency control considering governor dead-band and generation rate constraint. IEEE Trans Energy Convers 10(3): 555–561
19. Ramakrishna KSS, Bhatti TS (2008) Automatic generation control of single area power system with multi-source power generation. Proc Inst Mech Eng Part A J Power Energy 222(1):1–11
20. Tripathy SC, Balasubramanian R, Nair PSC (1992) Effect of superconducting magnetic energy storage on automatic generation control considering governor dead-band and boiler dynamics. IEEE Trans Power Syst 7(3):1266–1273
21. Park J, Sandberg IW (1991) Universal approximation using radial-basis-function networks. Neural Comput 3(2):246–257
22. Wu YL, Sun FC, Zheng JC, Song Q (2010) A robust training algorithm of discrete-time MIMO RNN and application in fault tolerant control of robotic system. Neural Comput Appl 19(7): 1013–1027
23. Chen S, Cowan CFN, Grant PM (1991) Orthogonal least squares learning algorithm for radial basis function networks. IEEE Trans Neural Netw 2(2):302–309